PHYSICAL REVIEW A **80**, 011813(R) (2009)

Single structured light beam as an atomic cloud splitter

B. M. Rodríguez-Lara* and R. Jáuregui†
Instituto de Física, Universidad Nacional Autónoma de México, Apdo. Postal 20-364, México Distrito Federal 01000, Mexico
(Received 26 March 2009; published 31 July 2009)

We propose a scheme to split a cloud of cold noninteracting neutral atoms based on their dipole interaction with a single structured light beam which exhibits parabolic cylindrical symmetry. Using semiclassical numerical simulations, we establish a direct relationship between the general properties of the light beam and the relevant geometric and kinematic properties acquired by the atomic cloud as it passes through the beam.

DOI: 10.1103/PhysRevA.80.011813 PACS number(s): 42.50.Tx, 37.10.Vz, 06.30.Ka

An optimal implementation of an atomic thermal cloud splitter requires achievement of a predetermined efficiency and deviation angle, as well as prevention of heating processes. Optical devices for splitting a free falling atomic cloud usually rely on two or more noncollinear [1] or collinear [2] light beams since a single Gaussian laser beam orthogonal to the falling atoms yields deviations of only some 10 mrad [3]. On chip, optical splitting requires either a pulse sequence of tightly linearly polarized beams [4] or the splitting into two of a former one-well dipole trapping beam via acousto-optical modulation [5]. It is also possible to use on chip magnetic fields to split the atomic cloud by including current carrier wires with varying bias or distance between them [6,7].

Here, we propose to reconsider the simple configuration of a single but *structured* laser beam orthogonal to a free falling atomic thermal cloud. Light beams with special intensity or phase structure yielding peculiar dynamical properties have been extensively used for the manipulation of microparticles [8] and cold atoms [9]. Most theoretical and experimental studies for cold atoms focus on using such light beams as wave guides for atom transport with the possibility of exchanging orbital angular momentum [9–16] or other dynamical properties [17] between the light and the atoms. We shall show that experimentally accessible structured light beams can also be used efficiently as atomic thermal cloud splitters. This proposal is based on semiclassical calculations that allow an estimate of the relevant geometrical and mechanical properties of the atomic cloud, such as deviation angles and kinetic energy, in terms of the atomic and light beams setup. In these calculations, the center of mass motion of each atom is described using Newtonian mechanics with the optical force derived from quantum theory [27].

The structured light beams we study are known as vector Weber beams. Under ideal conditions, the intensity pattern of an electromagnetic (em) Weber beam is invariant along the main direction of propagation. Its transverse structure is naturally described in terms of parabolic coordinates u and v related to the Cartesian coordinates through the equations $x=(u^2-v^2)/2$, $y=uv$, $u\epsilon(-\infty,\infty)$, and $v\epsilon[0,\infty)$. Its associated electric and magnetic fields can be written as a superposition of transverse electric (TE) and transverse magnetic (TM) modes [18]

$$\begin{aligned} \boldsymbol{E}_\kappa &= -\partial_{ct}(\mathcal{A}^{(\mathrm{TE})}\mathbb{M} - \mathcal{A}^{(\mathrm{TM})}\mathbb{N})\Psi_\kappa, \\ \boldsymbol{B}_\kappa &= \partial_{ct}(\mathcal{A}^{(\mathrm{TE})}\mathbb{N} - \mathcal{A}^{(\mathrm{TM})}\mathbb{M})\Psi_\kappa. \end{aligned} \tag{1}$$

The vector operators $\mathbb{M}$ and $\mathbb{N}$ are

$$\begin{aligned} \mathbb{M} &= h^{-1}\partial_{ct}(\boldsymbol{e}_u\partial_v - \boldsymbol{e}_v\partial_u), \\ \mathbb{N} &= h^{-1}\partial_z(\boldsymbol{e}_u\partial_u + \boldsymbol{e}_v\partial_v) - \boldsymbol{e}_z\nabla_\perp^2, \end{aligned} \tag{2}$$

where $h=\sqrt{u^2+v^2}$ denotes the scaling factor, $\boldsymbol{e}_\zeta$, $\zeta=u, v, z$ are the unitary vectors corresponding to parabolic-cylindrical coordinates, and the shorthand notation ∂_x is used for partial derivatives with respect to the variable x. The scalar field Ψ_κ is the solution of the wave equation:

$$\begin{aligned} \Psi_\kappa(u,v,z,t) &= \psi_{\mathfrak{p},k_\perp,a}(u,v)e^{i(k_z z-\omega t)} \\ &= \tilde{U}_{\mathfrak{p},k_\perp,a}(u)\tilde{V}_{\mathfrak{p},k_\perp,a}(v)e^{-i(k_\perp(u^2+v^2)/2+k_z z-\omega t)}, \end{aligned} \tag{3}$$

where

$$\begin{aligned} \tilde{U}_{\mathfrak{p},k_\perp,a}(u) &= (k_\perp u^2)^{n_\mathfrak{p}-1/4}{}_1F_1\left(\frac{n_\mathfrak{p}}{4} - i\frac{a}{2}, \frac{n_\mathfrak{p}}{2}; ik_\perp u^2\right), \\ \tilde{V}_{\mathfrak{p},k_\perp,a}(v) &= (k_\perp v^2)^{n_\mathfrak{p}-1/4}{}_1F_1\left(\frac{n_\mathfrak{p}}{4} + i\frac{a}{2}, \frac{n_\mathfrak{p}}{2}; ik_\perp v^2\right), \end{aligned}$$

with $n_\mathfrak{p}=1$ ($n_\mathfrak{p}=3$) for even (odd) parity functions and ${}_1F_1(x_1,x_2,x_3)$ is the confluent hypergeometric function directly related to Weber functions [19–21]. Up to a normalization factor, the scalar wave function $\psi_{\mathfrak{p},k_\perp,a}$ in terms of the Weber beam angular spectra $\mathfrak{U}$ is given by [22]

$$\psi_{\mathfrak{p},k_\perp,a}(x,y) = \int_{-\pi}^{\pi} \mathfrak{U}_\mathfrak{p}(a;\varphi)e^{-ik_\perp(x\cos\varphi + y\sin\varphi)}d\varphi, \tag{4}$$

$$\mathfrak{U}_e(a;\varphi) = \frac{e^{ia\ln|\tan\varphi/2|}}{2\sqrt{\pi\sin\varphi}}, \tag{5}$$

$$\mathfrak{U}_o(a;\varphi) = \begin{cases} i\mathfrak{U}_e(a;\varphi) & \varphi\epsilon(-\pi,0) \\ -i\mathfrak{U}_e(a;\varphi) & \varphi\epsilon(0,\pi). \end{cases} \tag{6}$$

The labels set $\kappa=\{\mathfrak{p},k_z,\omega,a\}$ in Eq. (1) refers to the mathematical parity, $\mathfrak{p}$ even or odd, z component of the wave vector, k_z, frequency, $\omega=ck=c\sqrt{k_z^2+k_\perp^2}$, and continuous order, $a\in\mathbb{R}$. The Weber beam transverse structure exhibits extended zones where the field has zero or close to zero values as illustrated in Fig. 1. For the order parameter $a\neq 0$, the low intensity zone is to the right (left) depending on the parameter a being negative (positive); its area increases in size as

*bmlara@fisica.unam.mx
†rocio@fisica.unam.mx

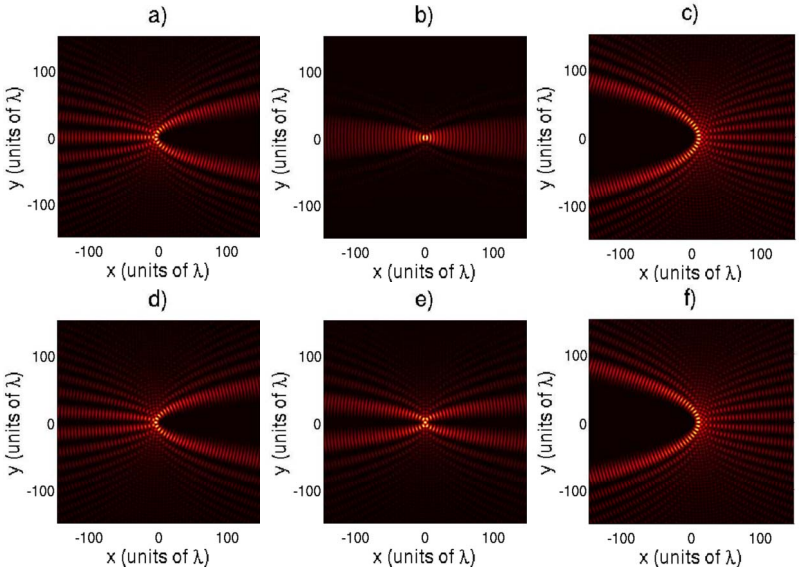

FIG. 1. (Color online) Sampler of the transverse structure of the intensity of Weber em fields as defined by Eqs. (1). Even/odd em Weber fields with eigenvalues (a/d) $a=-2$, (b/e) $a=0$, and (c/f) $a=5$.

the absolute value of a increases in magnitude. This dark region is approximately delimited by the parabola $y=\sqrt{2u_M^2(|x|-u_M^2/2)}$, where u_M is the value of u at the first maxima of the function $U_{\mathrm{p},k_\perp,a}(u)$. In Fig. 2, u_M as a function of a is illustrated.

The dynamical constants of Weber photons are the following [23]: its momentum along z, $\hbar k_z$, its energy $\hbar\omega$, and its eigenvalue, $\hbar^2 k_\perp a$, for the quantum operator

$$\hat{\mathbb{A}}_{\mathrm{em}}=\hbar\sum_{i=1}^{3}\int dV\hat{E}_i\frac{(l_z p_y+p_y l_z)}{2}\hat{A}_i=\sum_{i,\kappa}\hbar^2 k_\perp a\hat{N}_\kappa^{(i)}. \quad (7)$$

Here $\hat{N}_\kappa^{(i)}$ denotes the number operator of the κ mode, $l_z=-i(\vec{r}\times\vec{\nabla})_z$ as the generator of rotations along the z axis, and $p_y=-i\partial_y$ as the generator of translations along the y axis. Then, it would be said that the parameter a determines the product of the angular momentum along z and the momentum along y of a Weber photon whenever it could be shown that charged particles exchange that mechanical property with those photons.

Recently, Weber beams of zero order were experimentally generated by means of a thin annular slit modulated by the proper angular spectra [24]. This setup was conceived as a variation in that originally used by Durnin *et al.* [25] for generating Bessel beams. Higher-order Weber beams can be produced using holograms encoded either on plates [24] or on spatial light modulators [26].

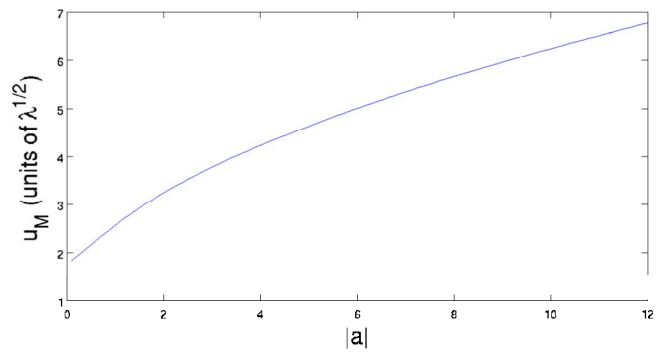

FIG. 2. (Color online) Value for u_M, the coordinate that defines the parabola delimiting the low intensity region of a Weber field, as a function of the eigenvalue a. The length unit was taken as the wavelength of the beam and $k_z=0.995k$.

The interaction between a two level atom and an em Weber wave with a frequency close to resonance is determined by the coupling factor

$$g^{\pm}=\boldsymbol{\mu}_{12}^{\pm}\cdot\boldsymbol{E}=\frac{\mu^{\pm}k}{h^2}(u\pm\imath v)(k\mathcal{A}^{(\mathrm{TE})}\mp\imath k_z\mathcal{A}^{(\mathrm{TM})})$$
$$\times(\partial_v\mp\imath\partial_u)\Psi_\kappa,$$

where the $\pm$ super index refers to the two possible cases for the atomic dipole transition element $\boldsymbol{\mu}_{12}^{\pm}=\mu_{12}^{\pm}(\boldsymbol{e}_x\pm\imath\boldsymbol{e}_y)$. In a semiclassical treatment, the gradient of g, $\boldsymbol{\nabla}g=(\boldsymbol{\alpha}+i\boldsymbol{\beta})g$, defines the force experienced by the atom. The expression for the average semiclassical velocity-dependent force valid for both propagating and standing beams is [27]

$$\langle\boldsymbol{f}\rangle=\frac{\hbar\Gamma[[(D(1-p)\boldsymbol{v}\cdot\boldsymbol{\alpha})+\Gamma/2]\boldsymbol{\beta}+[(\boldsymbol{v}\cdot\boldsymbol{\beta})-\delta\omega]\boldsymbol{\alpha}]}{(1-p')p'^{-1}\Gamma+2D\boldsymbol{v}\cdot\boldsymbol{\alpha}[1-p/p'-p]}, \quad (8)$$

with Γ is the Einstein coefficient, $\Gamma=4k^3|\boldsymbol{\mu}_{12}|^2/3\hbar$, $\delta\omega$ is the detuning between the wave frequency ω and the transition frequency ω_0, $\delta\omega=\omega-\omega_0$, $p=2|g|^2/[(\Gamma/2)^2+\delta\omega^2]$ is a saturation parameter linked to the difference D between the populations of the atom two levels, $D=1/(1+p)$, and finally $p'=2|g|^2/|\gamma'|^2$, with $\gamma'=(\boldsymbol{v}\cdot\boldsymbol{\alpha})(1-p)(1+p)^{-1}+\Gamma/2+\imath[-\delta\omega+(\boldsymbol{v}\cdot\boldsymbol{\beta})]$.

Our proposed scheme is focused on the red-detuned far off-resonance case so that nonconservative terms arising from the velocity dependence of the force are not dominant [28]. Nevertheless, we keep the velocity-dependent terms in the numerical calculations in order to prevent disregarding potentially relevant effects since the atom may increase its kinetic energy as it interacts with the light beam. The numerical simulations consider a TE laser beam detuned 67 nm to the red of the $5\ ^2S_{1/2}$-$5\ ^2P_{1/2}$ transition at 795 nm of ^{85}Rb with irradiance in the range of $\sim 1.5-6$ W/cm^2. As natural

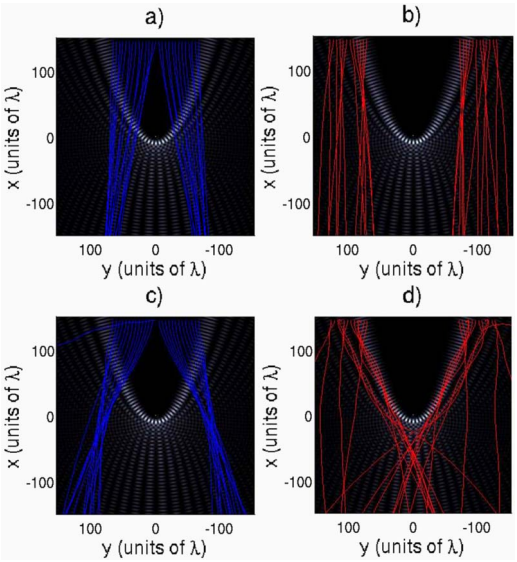

FIG. 3. (Color online) Evolution of an atomic cloud as it interacts with an odd TE Weber beam whose intensity pattern is illustrated in black and white. The atoms initial velocities are mainly in the direction of the gravitational field, $v_x \sim -0.6m\lambda\Gamma$ with random v_y and v_z components, $|v_x| \geq 10v_\perp$, corresponding to $T \sim 1.5$ μK. The Weber beam is characterized by $a=-5$, $k_z=0.995k$, and irradiance [(a) and (b)] 1.725 and [(c) and (d)] 6 W/cm^2. The atoms motion takes place within a $\sim 20\lambda$ wide region in the z axis.

length and time units, we take the laser wavelength and the inverse of the Einstein coefficient Γ, which is 3.7×10^7 s^{-1} for the state $5\ ^2P_{1/2}$ of ^{85}Rb.

An atomic cloud is released into a region where a Weber beam propagating in the horizontal direction was generated. The atoms have an initial velocity oriented by the gravitational field in the negative x direction, with a random smaller component in the y or z direction [we shall take $|v_x| \geq 10v_\perp = 10(v_y^2+v_z^2)^{1/2}$]. The Weber parameter a is taken negative so that, initially, the atomic cloud faces the low intensity region; for $x>0$, due to the red detuning of the light, the atoms that arrive in the dark region of the beam are attracted toward the delimiting parabola mentioned above and the splitting of the cloud takes place. In the region $x<0$ these atoms find a series of effective potential well channels that give rise to their focusing toward those channels. The atoms that arrive to the Weber beam outside the central dark region experience either a strong deflection when their initial position is on the bright parabolas or a weak deflection if their initial position is outside those parabolas. This behavior was found to be generic in all numerical simulations we performed. For the parameters mentioned above and $mv_x^2/2k_B \sim 1$ μK, the irradiance can be chosen so that the maximum deflection angle for the atoms that arrive in the dark region is $\theta_d^{\max} \sim \arctan\{[u_M^2/|x_0|(1-u_M^2/2|x_0|)]^{1/2}\}$, where x_0 is the initial atom x coordinate and u_M is the coordinate that defines the parabola delimiting the dark region; u_M is determined by the a parameter of the Weber beam [Fig. 2]. As expected, higher (lower) initial atomic kinetic energies require higher (lower) irradiance to achieve such deflection angles.

These results are illustrated in Fig. 3 for $a=-5$ and $x_0=150\lambda$. If $mv_x^2/2k_B \sim 1.5$ μK and the irradiance is 1.725 W/cm^2, the atoms that arrive to the beam within a distance of $\sim\lambda$ to the x axis are violently deflected, while those arriving in a zone $\lambda<|y|<2u_M^2 \sim 50\lambda$ have deflection angles up to $\theta_d^{\max} \sim 0.17$ rad [Fig. 3(a)]; those arriving at $80\lambda<|y|<150\lambda$ move almost vertically [Fig. 3(b)]. If the irradiance is almost quadrupled the deflection angle reach values of the order $\theta_d^{\max} \sim 0.35$ rad for atoms arriving at the dark zone [Fig. 3(c)], while the atoms arriving at $80\lambda<|y|<120\lambda$ are partially focused toward the x axis [Fig. 3(d)]. This effect is also interesting by itself since it could be used for merging independent clouds. In Fig. 4(a), the deflection angle, θ_d, is illustrated for all arriving zones. Typical values of θ_d are tenths of radians for atoms arriving at the dark zone of the beam.

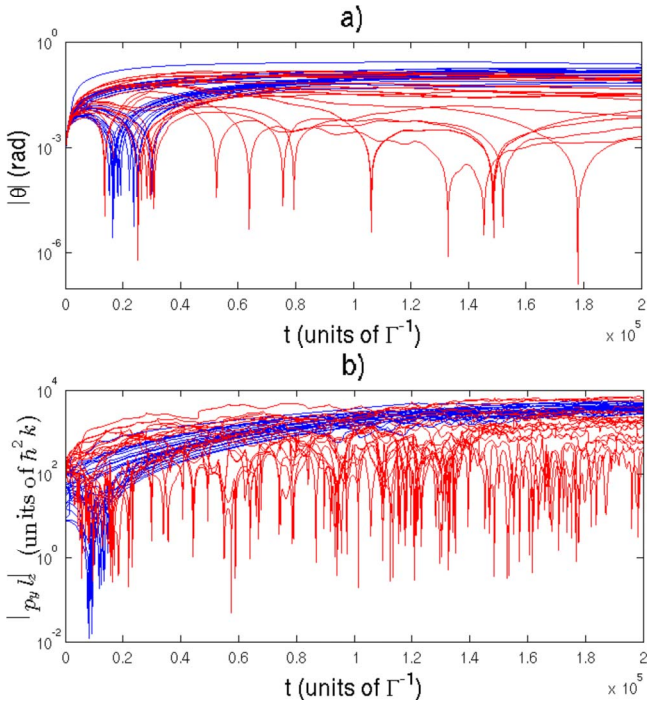

FIG. 4. (Color online) (a) Absolute value of the deviation angle, $\theta=\arctan y/x$ and (b) temporal evolution for the values of the mechanical property $\mathbb{A}_{\text{atomic}}=L_zP_y$ for different components of the clouds presented in Figs. 3(a) and 3(b).

Due to the parabolic symmetry of the problem, the product of the atomic angular momentum L_z and the linear momentum component P_y, $\mathbb{A}_{\text{atomic}}=L_zP_y$, is a relevant dynamical property for the description of the atomic cloud. As mentioned above, Weber beams carry a well-defined value of the similar em property $\mathbb{A}_{\text{em}}$ [Eq. (7)]. Through its classical motion, each atom locally detects the density $d\mathbb{A}_{\text{em}}/dV$, and could modify its $\mathbb{A}_{\text{atomic}}$ value. For the examples illustrated in Figs. 3(a) and 3(b), initially the atoms have $\mathbb{A}_{\text{atomic}}(0) \leq 150\hbar^2k_\perp$ and finally highly deflected atoms have $10^3\hbar^2k_\perp < \mathbb{A}_{\text{atomic}} < 10^4\hbar^2k_\perp$ as shown in Fig. 4(b). A detailed analysis lets us see that atoms arriving outside the dark beam region may exhibit high fluctuations in their $\mathbb{A}_{\text{atomic}}$ value as a function of time, while atoms focused into the same bright parabola for $x<0$ have similar asymptotic $\mathbb{A}_{\text{atomic}}$ values. These results show that Weber photons may transfer the dynamical variable $\mathbb{A}$ to atoms.

As for the kinetic energy acquired by the atoms, we divide it in two parts: the contribution due to the velocity in the gravitational direction $K_x = mv_x^2/2$ and that in the transverse direction $K_{yz} = mv_\perp^2/2$. For the example illustrated in Fig. 5(a), initially $K_x(0)/k_B \sim 1.5$ μK and $K_{yz}(0)/k_B \sim 0.02$ μK finally $K_x/k_B \sim 20$ μK and $K_{yz}/k_B(0) < 1$ μK for atoms arriving at the dark region, and $K_{yz}(0)/k_B \sim 1$ μK for atoms arriving in the other regions. The movement in the x direction is mainly driven by the gravitational field. The spreading in the kinetic energies is smaller for atoms arriving at the dark zone. At short times, $0 < t < 1.5 \times 10^4 \Gamma$, $|v_x|$ diminishes while in the average $v_\perp \sim |v_y|$ increases. That is, the atomic deflection takes place mainly in that time interval. Thus, if smaller final kinetic energy for the atoms is desired, the region of the optical field could be shortened along the x axis once the atomic thermal cloud has been split.

Summarizing, we have presented a scheme to split a cold noninteracting atomic cloud using a single Weber beam. This scheme requires no further optics or electronics but that used to generate the Weber beam. The atomic deflection angles are a function of the Weber parameter a and the irradiance of the beam, as well as the initial kinetic energy and arriving zone of the atoms. We have shown numerically that it is possible to manipulate the population of the split components of the atomic cloud through the control of the entry point of the cloud with respect to the center of symmetry of the em field intensity pattern. In fact, we have shown that this arrival dependence may be used to convert the light beam into a merging device. The atoms when guided by a parabolic bright region of the beam acquire values of $\mathbb{A}_{\text{atomic}} = L_z P_y$ with small dispersion. The main source of kinetic energy for the atoms is provided by the gravitational field.

For atoms that initially have kinetic energies in the quantum regime, lower irradiance of the light beam is expected to achieve similar deflection angles as those reported here. Under such conditions, studies on the quantum evolution in phase space of the atomic beam and its consequences on interferometric experiments would be especially interesting due to the topological structure of the em Weber field [23].

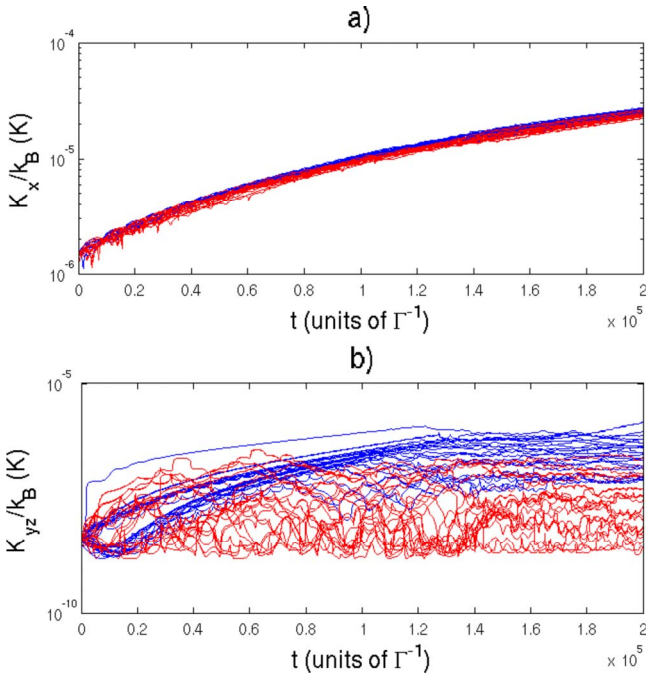

FIG. 5. (Color online) Contribution to the kinetic energy from (a) velocities parallel to the gravitational force direction, $K_x/k_B = mv_x^2/2k_B$ and (b) velocities perpendicular to the gravitational force direction, $K_{yz}/k_B = mv_\perp^2/2k_B$, for different components of the clouds presented in Figs. 3(a) and 3(b).

[1] O. Houde *et al.*, Phys. Rev. Lett. **85**, 5543 (2000).
[2] P. J. Martin *et al.*, Phys. Rev. Lett. **60**, 515 (1988); D. M. Giltner *et al.*, Phys. Rev. A **52**, 3966 (1995); M. K. Oberthaler *et al.*, Phys. Rev. Lett. **77**, 4980 (1996); S. Kunze *et al.*, Europhys. Lett. **34**, 343 (1996); M. Kozuma *et al.*, Phys. Rev. Lett. **82**, 871 (1999).
[3] F. Riehle *et al.*, Phys. Rev. Lett. **67**, 177 (1991); D. S. Weiss *et al.*, *ibid.* **70**, 2706 (1993); T. Pfau *et al.*, *ibid.* **71**, 3427 (1993); M. Weitz *et al.*, *ibid.* **73**, 2563 (1994); M. Weitz *et al.*, *ibid.* **77**, 2356 (1996).
[4] Y. J. Wang *et al.*, Phys. Rev. Lett. **94**, 090405 (2005).
[5] T. A. Pasquini *et al.* J. Phys.: Conf. Ser. **19**, 139 (2005).
[6] S. Kraft *et al.*, Eur. Phys. J. D **35**, 119 (2005).
[7] P. Hommelhoff *et al.*, New J. Phys. **7**, 3 (2005).
[8] K. Dholakia and W. M. Lee, Adv. At., Mol., Opt. Phys. **56**, 261 (2008).
[9] M. F. Andersen *et al.*, Phys. Rev. Lett. **97**, 170406 (2006); R. Pugatch *et al.*, *ibid.* **98**, 203601 (2007); D. Moretti *et al.*, Phys. Rev. A **79**, 023825 (2009).
[10] L. Allen *et al.*, Phys. Rev. A **45**, 8185 (1992).
[11] J. W. R. Tabosa and D. V. Petrov, Phys. Rev. Lett. **83**, 4967 (1999).
[12] M. Babiker *et al.*, Phys. Rev. Lett. **89**, 143601 (2002).
[13] G. S. Paraoanu, Phys. Rev. A **67**, 023607 (2003).
[14] H. L. Haroutyunyan and G. Nienhuis, Phys. Rev. A **70**, 063408 (2004).
[15] M. Bhattacharya, Opt. Commun. **279**, 219 (2007).
[16] K. Volke-Sepúlveda and R. Jáuregui, J. Phys. B **42**, 085303 (2009).
[17] B. M. Rodríguez-Lara and R. Jáuregui, Phys. Rev. A **78**, 033813 (2008).
[18] J. A. Stratton, *Electromagnetic Theory* (McGraw-Hill, New York, 1941).
[19] N. N. Lebedev, *Special Functions and their Applications* (Dover Publications, New York, 1972).
[20] M. Abramowitz and I. A. Stegun, *Handbook of Mathematical Functions* (Dover Publications, New York, 1972).
[21] K. Volke-Sepúlveda and E. Ley-Koo, J. Opt. A, Pure Appl. Opt. **8**, 867 (2006).
[22] M. Bandres *et al.*, Opt. Lett. **29**, 44 (2004).
[23] B. M. Rodríguez-Lara and R. Jáuregui, Phys. Rev. A **79**, 055806 (2009).
[24] C. López-Mariscal *et al.*, Opt. Express **13**, 2364 (2005).
[25] J. Durnin *et al.*, Phys. Rev. Lett. **58**, 1499 (1987).
[26] R. Ponce-Díaz *et al.*, Proc. SPIE **6311**, 63110D (2006).
[27] J. P. Gordon and A. Ashkin, Phys. Rev. A **21**, 1606 (1980).
[28] J. D. Miller *et al.*, Phys. Rev. A **47**, R4567 (1993).